TRENDS IN SCIENCES 2026; 23(7): 12660
https://doi.org/10.48048/tis.2026.12660
RESEARCH ARTICLE

Microwave-Activated Biomass-Derived Carbon for Smart Sensor Applications in Pollutant Detection and Drinking Water Purification

Agus Subagio[1,*], Risma Aimatul Qudsiyah[1], Heydar Ruffa Taufiq[1], Ngurah Ayu Ketut Umiati[1], Ida Hamidah[2], Ahmad Nurrudin[3] and Andrivo Rusydi[4]

[1]*Department of Physics, Faculty of Science and Mathematics, Universitas Diponegoro, Semarang 50275, Indonesia*
[2]*Department of Mechanical Engineering Education, Indonesia University of Education, Bandung 40154, Indonesia*
[3]*Faculty of Industrial Technology, Institut Teknologi Bandung, Bandung 40132, Indonesia*
[4]*Faculty of Science, National University of Singapore, Singapore 117546, Singapore*

([*]Corresponding author's e-mail: agussubagio@lecturer.undip.ac.id)

Received: 14 November 2025, Revised: 7 December 2025, Accepted: 20 December 2025, Published: 20 February 2026

Abstract

The increasing demand for sustainable materials in environmental monitoring has encouraged the use of biomass waste for the development of advanced sensor technology and water purification. This study reports the synthesis of activated carbon (AC) from tea stem biomass through activation with a microwave at 800 W for 120, 180, and 240 s. The variation in time was used to investigate the effect of activation time on structure, porosity, and electrochemical performance. X-ray diffraction confirmed a progressive transition from predominantly amorphous carbon at 120 s to a more regular graphite structure at 180 - 240 s. AC Tea Waste 180 s showed a balanced degree of crystallinity without significant structural fragmentation. SEM analysis showed that 180 s of activation resulted in a highly open and interconnected pore network, while shorter activation resulted in relatively closed pores, and longer activation caused surface cracks and particle fragmentation. Electrochemical testing in a 1 M Na_2SO_4 solution using a three-electrode configuration showed that AC activated for 180 s produced the highest specific capacitance of 735.76 F g^{-1} at a current of 2.5 A g^{-1}, accompanied by better rate capability and lower charge transfer resistance compared to the 120- and 240- s samples. At the same activation time, the material achieved an energy density of 366.41 Ws g^{-1} at a power density of 0.875 W g^{-1}, demonstrating a balance between energy and power for practical applications. The optimized AC exhibits a characteristic quasi-rectangular cyclic voltammetry profile of electrochemical double-layer capacitance, stable charge-discharge behavior, and favorable ion transport, confirming its suitability as a supercapacitor transducer layer. Furthermore, the high carbon purity and tailored pore structure of the 180 s sample provide strong sensitivity for pollutant detection and robust adsorption capacity for drinking water purification, demonstrating that tea stalk waste is a low-cost, renewable raw material for multifunctional smart sensors and clean water technology.

Keywords: Microwave activation, Biomass-derived carbon, Pollutant detection, Water purification, Smart sensor

Introduction

The increasing global population has led to a surge in food consumption and agricultural production, resulting in a rapid accumulation of agricultural waste (AW). AW, particularly lignocellulosic biomass, is rich in cellulose (30% - 40%), hemicellulose (30% - 50%), and lignin (8% - 21%), making it a promising and sustainable carbon source for advanced environmental applications [1]. The valorization of biomass waste into value-added products, such as activated carbon, is gaining attention due to its potential to provide low-cost, eco-friendly materials for environmental monitoring and water purification [2].

Recent studies have demonstrated that activated porous carbon derived from environmental waste can be

tailored for various applications, including smart sensors and water treatment systems [3,4]. However, the development of new carbon materials must meet industry demands for sustainability, cost-effectiveness, and tunable properties such as high surface area, porosity, and electrochemical performance [5-7]. Despite these advances, there remains a critical gap in optimizing the synthesis process, particularly activation parameters, to maximize the functional performance of biomass-derived carbon for sensor and purification applications.

Tea stems have a lignocellulosic structure composed of an outer protective epidermis, a lignin-reinforced cortex, and a central vascular system [8]. The epidermis has a smooth structure and is covered with a thin cuticle that protects the tissue from moisture loss. Beneath it, the cortex contains parenchyma cells interspersed with sclerenchyma fibers, which provide rigidity and mechanical strength. This sclerenchyma tissue is rich in lignin, making the stem hard and woody in texture compared to tea leaves [9]. The vascular system, consisting of xylem and phloem, transports water and nutrients. The xylem vessels are relatively large and elongated, while the phloem tissue appears as smaller, denser clusters of cells around the vessels. The overall internal structure forms a dense, hierarchical lignocellulosic fiber network. When carbonized, this natural arrangement contributes to the formation of micro- to mesopores through the decomposition of hemicellulose and cellulose, while the lignin-rich areas form a stable carbon framework. The structure of tea stems makes them a suitable raw material for activated carbon, especially for applications that require good mechanical integrity and interconnected pore networks [10-13]. Microwave-assisted activation has emerged as a rapid, energy-efficient method to produce carbon materials with tunable pore structures and enhanced electrochemical properties [12,14,15]. Research conducted by Hu *et al*. [16] reinforces that microwave-based KOH activation can drastically improve pore structure and surface properties, making it highly relevant for producing activated carbon from biomass waste, including tea waste. Tea waste, which is rich in lignocellulose, has similar potential and can produce high-value activated carbon for energy and adsorption applications [16]. However, specific research on the effect of microwave activation time on the physicochemical and electrochemical characteristics of tea waste carbon is still limited, so further studies are needed to optimize the process and maximize its performance.

The characteristics of activated carbon can be adjusted by regulating the activator/carbon precursor ratio, the activation pyrolysis temperature, and activating agents such as $ZnCl_2$, $FeCl_3$, H_3PO_4, K_2CO_3, and KOH [14]. Carbon materials are electrically conductive, have low electrical resistance, a large specific surface area, and can physically absorb a large amount of charge onto their surface [12,15]. Due to their simplicity of synthesis, low cost, flexible pore design, and excellent chemical and thermal stability, porous activated carbon materials show tremendous potential for environmental applications [17,18].

H_3PO_4 was used as an activator in this study due to its ability to produce larger and more uniform pores, a rougher surface structure, and to maintain activated carbon with a higher yield and be more environmentally friendly than other activators such as $ZnCl_2$ or KOH. H_3PO_4 also produces phosphorus functional groups that enhance interaction with pollutants, and requires less energy and a more economical process than other activators. In addition, H_3PO_4 is easier to recover after the process, has a smaller environmental impact, and is capable of producing materials with high porosity that are very suitable for adsorption and water purification applications [19].

Based on the results of research by Yakout & Sharaf El-Deen [20] and Nimah *et al.* [21], carbon activation from waste biomass using microwave and H_3PO_4 methods has been proven to produce materials with high porosity, large surface area (818 - 1,218 m^2/g), and micro pore structures that are very effective for the adsorption of heavy metal contaminants and organic pollutants. The advantages of using the microwave method and H_3PO_4 activator are a fast, energy-efficient process, high adsorption capacity supported by a larger, cleaner, and more uniform pore structure, and the addition of functional groups that enhance interaction with pollutants. Previous studies have not systematically explored variations in carbonization time, and applications have been limited to conventional adsorption, so there has been no evaluation of the material's potential as a smart sensor or for specific drinking water purification. This research is crucial for

optimizing pore structure, expanding the material's multifunctional sensor capabilities, and improving efficiency and selectivity in sustainable drinking water purification, addressing the limitations of previous studies and opening innovation opportunities in the fields of biomass-based sensors and water purification.

Materials and methods

Chemicals and instrumentation

Chemicals used in this study include tea stem biomass as carbon precursor, phosphoric acid (H_3PO_4, analytical grade) from Merck (Darmstadt, Germany), polyvinylidene fluoride (PVDF, 99.5% purity), and dimethylformamide (DMF) solvent from Sigma-Aldrich (St. Louis, MO, USA). Aluminum foil (purity > 99%) was used as the substrate, and argon gas (99.99% purity) from Air Liquide was employed to maintain an inert atmosphere during microwave activation.

Characterizations were performed using X-ray diffraction (XRD, Rigaku MiniFlex 600, Cu Kα radiation, λ = 1.54 Å) was employed to determine the crystalline structure and phase composition of the materials. The surface morphology and microstructural features were examined using scanning electron microscopy (SEM, JEOL JSM-6510LV). Electrochemical performance was evaluated through cyclic voltammetry (CV), galvanostatic charge–discharge (GCD), and electrochemical impedance spectroscopy (EIS) to investigate the charge storage behavior, specific capacitance, and ion transport characteristics of the electrodes.

Synthesis of activated carbon from tea stem biomass

This study uses research conducted by Yakout *et al*. [20], which has been modified [20]. Tea stalk waste is dried under the sun. Then, it is cut into pieces and ground using a blender. Next, it is filtered to obtain the finest particles with a size of 180 µm. The tea stalk waste pulp solution was mixed with H_3PO_4 in a 3:1 ratio. Carbonization and activation with the aid of a microwave were carried out at 800 W power and carbonized at 3 different times, namely 120, 180, and 240 s under a continuous argon flow (50 mL min^{-1}). After that, the activated carbon was washed with 200 mL of distilled water to a neutral pH (~6.5) and dried at 80 °C for 2 h.

Fabrication of single electrodes

Fabrication of single electrodes using references from research conducted by Wang *et al*. [22], modified. Electrode slurry was prepared by dissolving 10 wt% PVDF binder in 10 mL of DMF, followed by stirring at 300 rpm for 1 h at room temperature. Activated carbon powder (90 wt%) was added and mixed under the same conditions for another hour. The resulting homogeneous slurry was coated onto aluminum foil substrates using the doctor blade method with a micrometer-adjustable film applicator to achieve a film thickness of approximately 25 µm. Electrode films were dried at 80 °C for 2 h.

Electrochemical characterization

Electrochemical properties were evaluated using cyclic voltammetry (CV), galvanostatic charge–discharge (GCD), and electrochemical impedance spectroscopy (EIS) on a PalmSens4 potentiostat controlled by PSTrace BETA 5.10 software. All tests were conducted in 100 mL of 1 M aqueous Na_2SO_4 electrolyte. A three-electrode configuration was used, with the synthesized carbon electrode as the working electrode, a platinum plate as the counter electrode, and an Ag/AgCl electrode as the reference electrode.

CV testing was carried out to analyze the capacitive behavior and charge storage mechanism of the electrodes by observing the cyclic curve profile in the potential range of 0 - 1 V at scan rates of 10, 25, 50, 75, and 100 mV s^{-1} over a potential range of -1.0 to 0.1 V at Na_2SO_4 electrolyte solution of 1 M.

The GCD measurements were performed at different current densities of 0.5, 1.0, 2.5, 5.0, 7.5, and 10.0 A g^{-1} to determine the specific capacitance (C_s), energy density (E), and power density (P) under various electrolyte concentrations using the following Eqs. (1) - (3) [23].

$$C_s = \frac{I \times \Delta t}{m \times \Delta V} \quad (1)$$

$$E = \frac{C_s \times \Delta V^2}{2 \times 3.6} \quad (2)$$

$$P = \frac{3600 \times E}{t} \quad (3)$$

where:
'I' is the current (A),
'ΔV' is a potential window (V),
'Δt' is the discharging time (s), and
'm' is the weight of the active electrode (g).

EIS analysis was conducted in the frequency range from 0.1 Hz to 10^6 Hz to study the internal resistance, charge transfer resistance, and ion diffusion behavior of the electrodes at different electrolyte molarities.

Results and discussion

Based on the XRD analysis results (**Figure 1**), activated carbon was synthesized from tea stalk waste with microwave activation times varying between 120, 180, and 240 s. The dominant peak observed at around 2θ = 24° - 25° (002) and 2θ = 24° - 25° (100) crystal plane of graphite carbon, in accordance with JCPDS reference number 00-041-148. Peaks 2θ = 12° and 15°, the peaks likely originate from partially degraded organic compounds (cellulose/hemicellulose/lignin) and hydrated minerals commonly found in tea biomass. Peaks 2θ = 17° and 20°, the presence of residual crystalline biopolymer structures indicates an incomplete carbonization process [24]. The peak at 2θ = 22° - 24° (002) appears with a low peak, indicating a very small crystalline domain size and a low order of active carbon layer stacking [25]. The peak at 2θ ≈ 37° is likely to originate from inorganic impurities [26].

The XRD results with an active carbonization time of 180 s show a significant reduction in peaks associated with the presence of impurities. Carbon begins to form, marked by the appearance of 2θ = 24° (002) and 27° (100). The structural state indicated by the XRD graph shows that amorphous carbon remains rich in surface functional groups, resulting in a favorable balance between porosity, irregularity, and electroactive sites. At 2θ = 32°, a minor peak indicates the presence of impurity phases carried over from precursors or activators [12,25,27].

The XRD results with an active carbonization time of 240 s show an activated carbon structure characterized by broad and intense peaks centered around 24° (002) with a secondary shoulder near 27° (100) and the disappearance of almost all previous sharp peaks. This indicates that microwave activation results in the formation of an optimal amorphous carbon network [12,28,29].

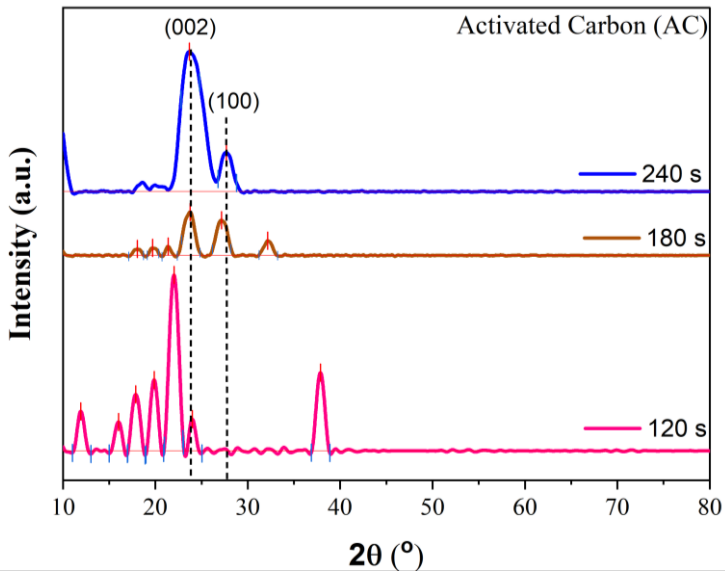

Figure 1 XRD patterns of activated carbon with carbonization times varying between 120s, 180s, and 240s.

However, extending the activation time to 240 s can also cause the structure to begin to fragment and reduce the mechanical strength of the material due to excessive crystal growth. Optimizing the activation time between 120 and 180 s produces activated carbon with a more balanced pore structure and crystallinity, which supports the best electrochemical performance as a biomass-based smart sensor electrode. In general, this

XRD pattern confirms the transition from an amorphous to a graphitic structure as the activation time increases, consistent with the characteristics of microwave-activated activated carbon [30].

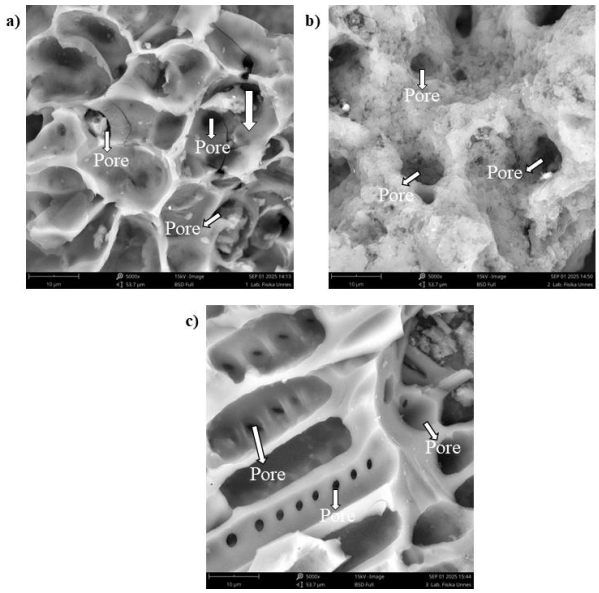

Figure 2 SEM results of activated carbon (AC) from tea stalk waste with varying microwave times. (a) 120 s, (b) 180 s, and (c) 240 s.

Morphological analysis using SEM on activated carbon synthesized from tea stalk waste with varying microwave activation times, as shown in **Figure 2**, reveals significant changes in the surface structure. At 120 s of activation, the surface of the activated carbon had fairly uniform pores with small sizes, indicating a relatively closed morphology. Increasing the activation time to 180 s resulted in a more open surface with larger and increased numbers of pores, describing an optimal pore structure for electrode applications. However, at 240 s of activation, although the pores remained clearly visible and large, the surface began to show a fragmented structure, which could reduce the mechanical strength and overall stability of the material.

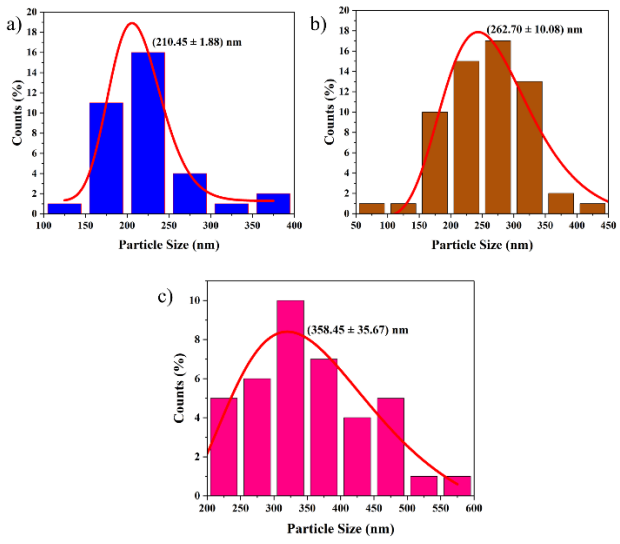

Figure 3 Distribution of activated carbon (AC) particle size from tea stalk waste with varying microwave times: (a) 120 s, (b) 180 s, and (c) 240 s.

The average particle size of activated carbon also increased from 210.45 nm at 120 s to 358.45 nm at 240 s, which was caused by an increase in crystallinity due to longer activation times. This analysis supports the importance of optimizing the activation time so that activated carbon has the porosity and structure that best supports electrochemical performance. These results are in line with the findings in an international journal by Vakili *et al*. [31], which show that too short an activation time results in an amorphous structure, and too long an activation time causes microstructure fragmentation, thereby reducing material performance [31].

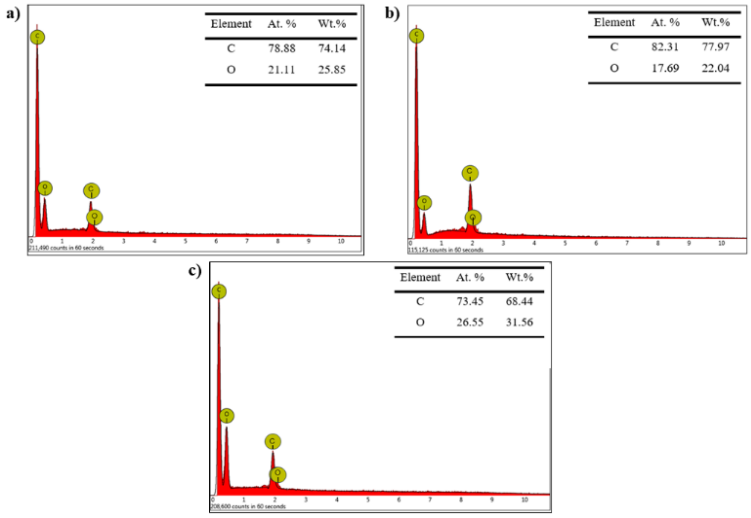

Figure 4 EDX results of activated carbon (AC) from tea stalk waste with varying microwave times: A) 120 s, b) 180 s, and c) 240 s

EDX analysis of activated carbon produced from tea stalk waste is shown in **Figure 4**. EDX analysis shows that all samples consist of carbon and oxygen components without any detectable metal contaminants, indicating high elemental purity suitable for adsorption and electrochemical applications. For material carbonized for 120 s, the carbon content reached 74.14% by weight (78.88% by atom), while oxygen was 25.85% by weight (21.11% by atom), indicating a carbon framework that was still rich in oxygen content.

After 180 s of carbonization, the carbon content increased to 77.97% by weight (82.31% by atom), accompanied by a decrease in oxygen to 22.04% by weight (17.69% by atom), indicating progressive deoxygenation and aromatization of the carbon matrix along with the removal of oxygen groups. In contrast, samples processed for 240 s showed slightly lower carbon content (68.44% by weight and 73.45% by atom) due to structural fragmentation or further oxidation caused by excessive activation time. The higher oxygen content (31.56% by weight and 26.55% by atom) was due to surface reoxidation, resulting in a higher oxygen content [32].

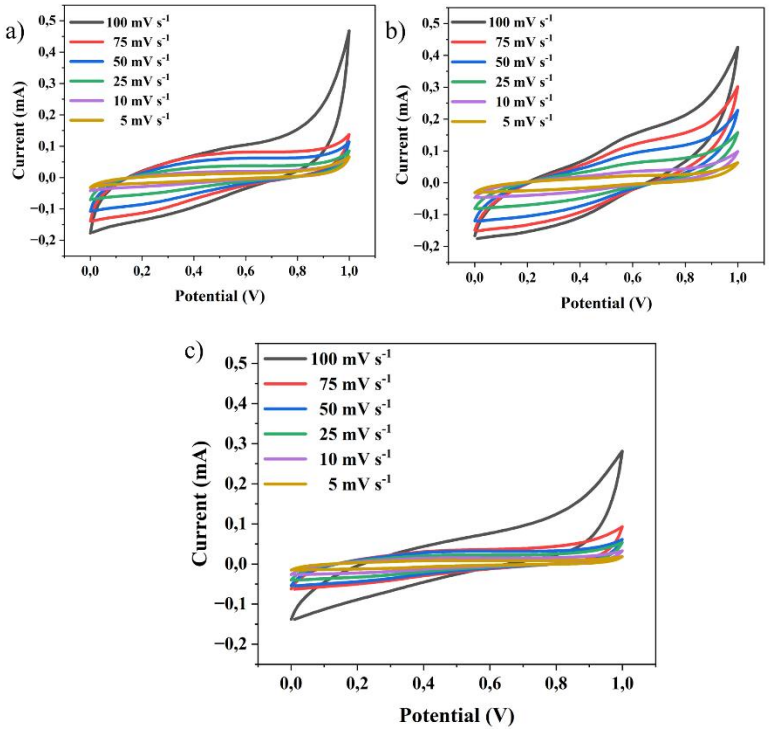

Figure 5 Supercapacitive behavior of electrodes at scan rates of 5 mV s^{-1}, 10 mV s^{-1}, 25 mV s^{-1}, 50 mV s^{-1}, 75 mV s^{-1}, 100 mV s^{-1} for AC variations in tea waste (a) 120 s, (b) 180 s, (c) 240 s.

Based on the curve shape in **Figure 5** from the Cyclic Voltammetry (CV) results of carbon from tea stalk waste, all graphs at varying deposition times (120 s, 180 s, 240 s) show a pattern characteristic of porous carbon materials, namely a quasi-rectangular shape in the voltage range between 0 and 1 V. This shape is characteristic of activated carbon materials that function as supercapacitor electrodes with an electrostatic charge storage mechanism (electrochemical double layer capacitance/EDLC). The absence of prominent redox peaks indicates that the dominant process is ion adsorption on the carbon surface, while the symmetry of the curve with respect to the current axis indicates a reversible process and good charge transfer efficiency [33-35].

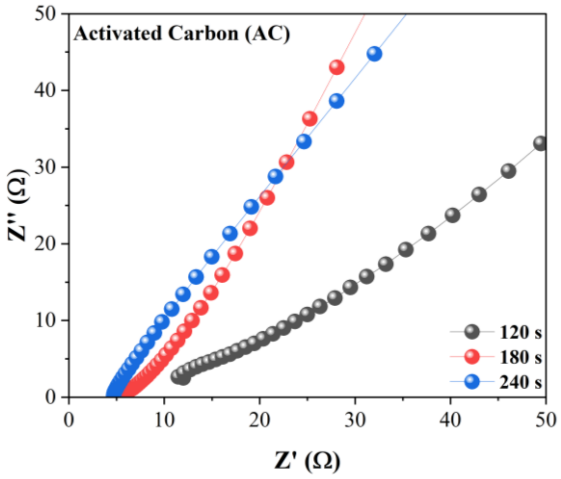

Figure 6 Nyquist plot and circuit fitting in the EIS test of a single activated carbon electrode at varying activation times at 120s, 180s, and 240s.

The next electrochemical test involved electrochemical impedance spectroscopy (EIS) analysis. The test was conducted using a three-electrode system, where the working electrode used the fabricated material, the counter electrode used platinum, and the reference electrode used Ag/AgCl. The electrolyte used was 1 M Na_2SO_4 at room temperature. The test was carried out using a fixed scanning scheme with a frequency range from 1 Hz to 100 kHz. The results of the EIS analysis in the form of a Nyquist plot and circuit diagram are shown in **Figure 6**. The Nyquist plot shows the electrochemical impedance response at various frequencies, while the circuit diagram provides information about the circuit elements that describe the electrochemical properties of the tested system.

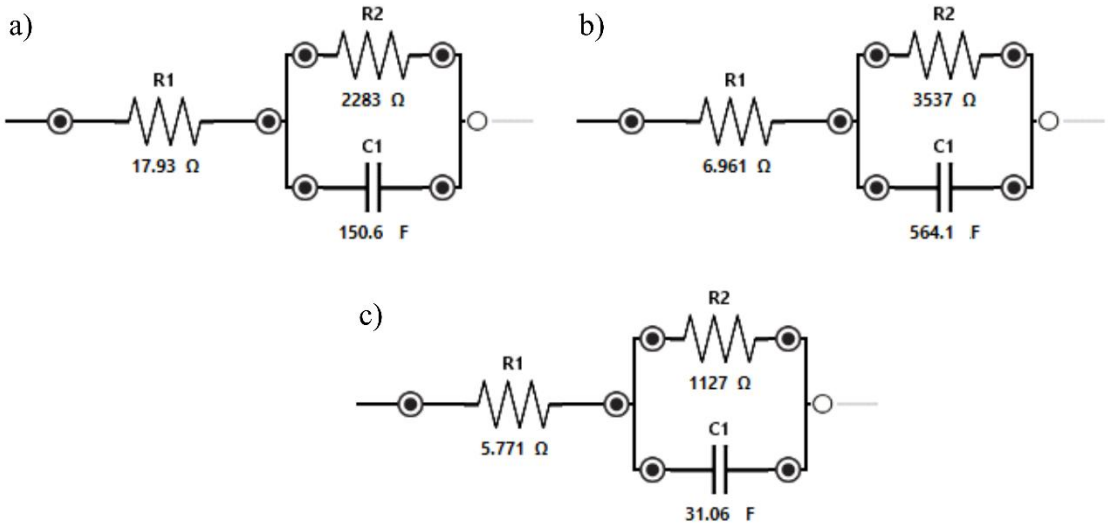

Figure 7 Randles plots from EIS testing of single activated carbon electrode materials at varying carbonization times: (a) 120 s, (b) 180 s, and (c) 240 s.

In the circuit adjustment results in **Figure 7** in the form of a randles circuit, the resistance value that appears in the circuit (circuit resistance) shown in **Table 1** shows an increase in resistance value proportional to the carbonization time. Research has shown that electrical resistivity generally decreases with increasing carbonization time, as the material becomes more graphitic and regular. For example, one study showed that as the regularity of the structure increased due to longer carbonization times, the resistivity value decreased significantly [36].

Table 1 Results of the Nyquist plot analysis that has been fitted to the circuit design.

Activation Time (s)	R_1 (Ω)	R_2 (Ω)	C_1 (F)
120	17.93	2283	150.6
180	6.961	3537	564.1
240	5.771	1127	31.06

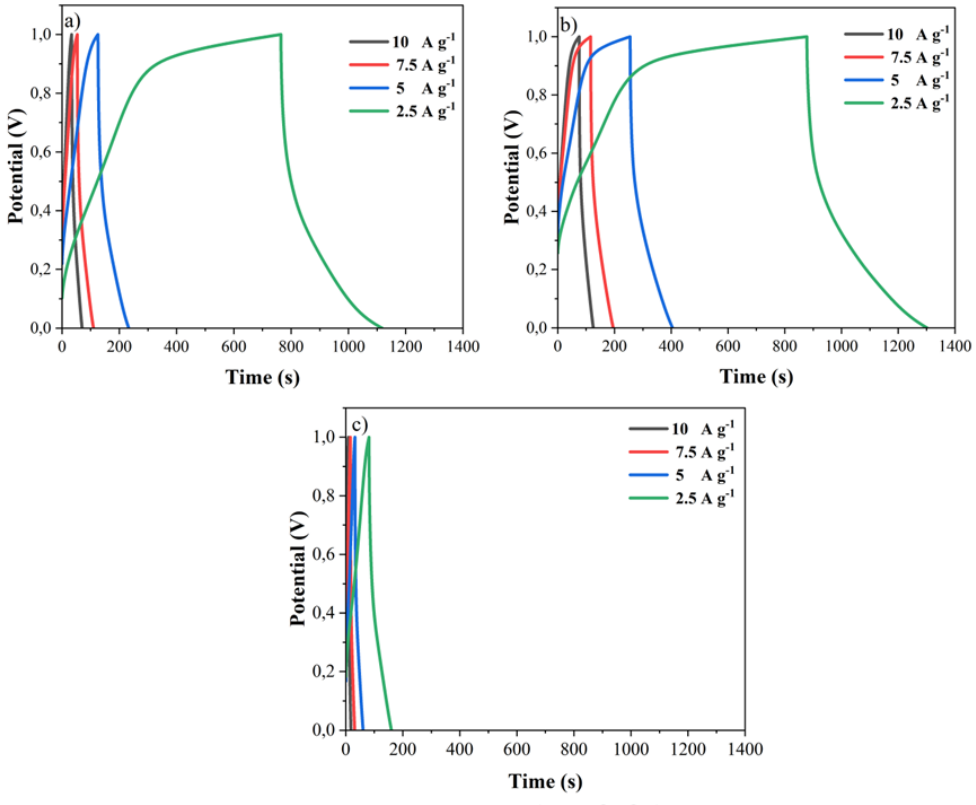

Figure 8 GCD analysis graph of tea waste carbon with varying activation times: (a) 120 s, (b) 180 s, and (c) 240 s.

The GCD carbon analysis graph of tea waste shown in **Figure 8** at different activation times, namely 120, 180, and 240 s, indicates that electrode performance is greatly influenced by the activation duration and test current magnitude. At 120 and 180 s of activation, the material showed higher storage capacity, especially at low currents of 2.5 A g^{-1}, which was characterized by longer discharge times. However, when the activation time was extended to 240 s, the discharge time was significantly reduced for all currents, indicating a decrease in specific capacitance, possibly due to an overdeveloped or collapsed pore structure that inhibited electrolyte ion diffusion [37,38]. Increased testing current causes shorter discharge times because ions cannot diffuse optimally into the electrode. The imperfect GCD curve with IR drop during the charge-discharge transition also indicates internal resistance in the material. Overall, these results emphasize the importance of optimizing activation time so that tea waste carbon can have a good pore structure, thereby maintaining maximum capacitance and efficiency as a smart sensor. Activation that is too short or too long can each cause low capacitance and a decrease in material performance as a single electrode in smart sensors. Therefore, an activation time between 120 and 180 s appears to be the optimal range for this application [37].

Table 2 Specific capacitance values of AC materials from tea waste based on GCD analysis.

Current Density (A g^{-1})	Spesific Capacitance (F g^{-1})		
	120 s	**180 s**	**240 s**
2.5	618.03	735.76	141.91
5	374.95	528.52	100.7
7.5	298.86	428.04	99.9
10	254.42	348.24	63.76

The specific capacitance (**Table 2**) of AC from tea waste was found to be 618.03, 735.76, and 141.91 F g^{-1} at a current density of 2.5 A g^{-1}. The results show that the optimal time used for carbon activation using the microwave irradiation method is 180s. It can be noted that accessible surface area is a key factor related to capacitance. A decrease in pore size and pore volume reduces electrochemical performance by reducing the active surface sites responsible for electron conduction during the electrochemical process

Table 3 Energy density and power density values for AC materials from tea waste based on GCD analysis.

Power Density (W g^{-1})	Energy Density (Ws g^{-1})		
	120 s	**180 s**	**240 s**
0.875	307.78	366.41	68.12
1,75	186.73	262.94	49.70
2,65	148.53	213.59	50.05
3.5	126.7	173.43	31.85

The results of energy density and power density data analysis on activated carbon from microwave activation of tea waste show that an activation time of 180 s is optimal, producing an energy density of 366.41 Ws g^{-1} at a power density of 0.875 W g^{-1}, which is much higher than other activation times. while increasing the time to 240 s causes a decrease in performance due to carbon structure fragmentation and loss of active pores necessary for charge storage. This trade-off phenomenon between power density and energy density is consistent with the characteristics of biomass-based activated carbon supercapacitors, namely that an increase in surface area and micro-pores during optimal activation increases energy capacity, but overexposure reduces performance. These results are in line with recent studies on biomass carbon electrodes and their applications in sensors and water purification, for example in the literature by Mehmandoust *et al*. [39] and Reddygunta *et al*. [40], which also emphasize that synthesis parameters are crucial in producing high-performance supercapacitor electrodes and sensors for sustainable applications in the environmental and energy fields [39,40].

Conclusions

Based on the results of this study, microwave activation of tea stalk waste produces porous activated carbon with superior electrochemical properties that are highly suitable for smart sensor and water purification applications; the optimal activation time was found to be 180 s, which provided the highest specific capacitance of 735.76 F g^{-1} at a current density of 2.5 A g^{-1}, well-developed pore structure, and high energy efficiency, while too short an activation duration produces low-performance amorphous carbon and excessive duration causes structural fragmentation and decreased performance; the optimized activated carbon exhibits high sensitivity to pollutant detection as well as strong adsorption power in water purification, thus having the potential as a multifunctional material that supports the integration of environmental and clean water sensor technologies in a sustainable manner; Overall, this study proves that tea stalk waste is a renewable and economical precursor for producing high-performance activated carbon using energy-efficient microwave irradiation, while also making a real contribution to the development of environmentally friendly material technologies and solutions for future water monitoring and purification.

Acknowledgements

The authors sincerely thank the Nanotechnology Laboratory for their support in material synthesis and testing throughout this research. Financial support was provided by the Institute for Research and Community Services, Universitas Diponegoro, through the RKI 2025 project #434-14/UN7.D2/PP/VI/2025.

Declaration of generative AI in scientific writing

The authors acknowledge the use of generative artificial intelligence tools (Preplexity) for language editing and grammar correction. No content generation or data interpretation was performed by artificial intelligence. The authors take full responsibility for the content and conclusions of this work.

CRediT author statement

Agus Subagio: Conceptualization, Methodology, Supervision, Review & Editing. **Risma Aimatul Qudsiyah:** Investigation, Resources, Validation, Software, Writing – Original Draft. **Heydar Ruffa Taufiq:** Investigation, Software, Writing – Review & Editing. **Ngurah Ayu Ketut Umiati:** Supervision, Software, Writing – Review & Editing. **Ida Hamidah:** Supervision, Formal Analysis. **Ahmad Nurrudin:** Data Curation. **Andrivo Rusydi:** Data Curation, Formal Analysis.

References

[1] LP Magagula, CM Masemola, MA Ballim, ZN Tetana, N Moloto and EC Linganiso. Lignocellulosic biomass waste-derived cellulose nanocrystals and carbon nanomaterials: A review. *International Journal of Molecular Sciences* 2022; **23(8)**, 4310.

[2] F Vallejo, D Yánez, L Díaz-Robles, M Oyaneder, S Alejandro-Martín, R Zalakeviciute and T Romero. Valorizing biomass waste: Hydrothermal carbonization and chemical activation for activated carbon production. *Biomass* 2025; **5(3)**, 45.

[3] MB Mosbah, L Mechi, R.Khiari and Y Moussaoui. Current State of Porous Carbon for Wastewater Treatment. *Processes* 2020; **8(12)**, 1651

[4] A Kumar, R Aslam, C Verma and OM Rodríguez-Narváez. *Activated carbon for environmental applications*. *In*: C Verma and MA Quraishi (Eds.). Activated carbon. The Royal Society of Chemistry, London, 2023, p. 70-91.

[5] AM Afridi, M Aktary, SS Shah, SM Sheikh, GJ Islam, MN Shaikh and MA Aziz. Advancing electrical engineering with biomass-derived carbon materials: Applications, innovations, and future directions. *The Chemical Record* 2024; **24(12)**, e202400144.

[6] RO Gembo, S Odisitse and CK King'ondu. Transforming waste resources into efficient activated carbon for energy storage and environmental remediation: A comprehensive review. *International Journal of Environmental Science and Technology* 2024; **21(7)**, 6167-6206.

[7] S Yarramsetti, M Girirajan, S Kalluri, S Sangaraju and PS Maram. Multifunctional activated carbon derived from novel biomass for high-performance energy storage applications: A sustainable alternative to fossil-fuel-derived carbon. *Materials Chemistry and Physics* 2024; **320**, 129424.

[8] P Das, V Chettri, S Ghosh and C Ghosh. Micromorphological studies of the leaf and stem of *Camellia sinensis* (L.) Kuntze with reference to their taxonomic significance. *Microscopy Research and Technique*; **86(4)**, 465-472.

[9] R Crang, S Lyons-Sobaski and R Wise. Parenchyma, collenchyma, and sclerenchyma. *Plant Anatomy* 2018. https://doi.org/10.1007/978-3-319-77315-5_6

[10] L Wu, D Xue, R Wen, X Jiang, L Jiao and H Chen. *Production of activated carbon from tea. Recent advances in activated carbon: Synthesis, properties and applications*. *In*: HS Min, HS Kusuma and YC Sharma (Eds.). Recent advances in activated carbon. CRC Press, Florida, 2024, p. 14.

[11] S Ahmed, Z Ferdous and Fatema-Tuj-Zohra. Prospective application of eco-friendly banana peel reduced graphene oxide (BRGO) for aqueous Cr (VI) and acid dye adsorption: A waste utilization approach. *Bioresource Technology Reports* 2024; **27**, 101936.

[12] AA Ahmad, M Al-Raggad and N Shareef. Production of activated carbon derived from agricultural by-products via microwave-induced chemical activation: A review. *Carbon Letters* 2021; **31(5)**, 957-971.

[13] X Qu, W Kang, C Lai, C Zhang and SW Hong. A simple route to produce highly efficient porous carbons recycled from tea waste for high-performance symmetric supercapacitor electrodes. *Molecules* 2022; **27**, 791.

[14] R Nandi, MK Jha, SK Guchhait, D Sutradhar and S Yadav. Impact of KOH activation on rice husk derived porous activated carbon for carbon capture at flue gas alike temperatures with high CO_2/N_2 Selectivity. *ACS Omega* 2023; **8(5)**, 4802-4812.

[15] IG Dyachkova, DA Zolotov, AS Kumskov, IS Volchkov, VV Berestov and EV Matveev. Possibilities of the microwave method for the activation of carbon materials in comparison with the traditional thermal method. *Physics-Uspekhi* 2023; **66(12)**, 1248-1257.

[16] W Hu, S Cheng, H Xia, L Zhang, X Jiang, Q Zhang and Q Chen. Waste phenolic resin derived activated carbon by microwave-assisted KOH activation and application to dye wastewater treatment. *Green Processing and Synthesis* 2019; **8(1)**, 408-415.

[17] R Kasana, U Shashikumar, CM Hussain and S Chawla. Green carbon materials for sensing applications. *ACS Symposium Series* 2023; **1441**, 163-179.

[18] AM Pai, MM Shanbhag, T Maiyalagan, SA Alqarni and NP Shetti. Activated carbon synthesized from *Arecanut catechu* L. as a sustainable precursor intercalated TiO_2 modified electrode for the detection of fungicide Dichlorophen. *Diamond and Related Materials*2023; **140(B)**, 110561.

[19] I Neme, G Gonfa and C Masi. Activated carbon from biomass precursors using phosphoric acid: A review. *Heliyon* 2022; **8(12)**, e11940.

[20] SM Yakout and G Sharaf El-Deen. Characterization of activated carbon prepared by phosphoric acid activation of olive stones. *Arabian Journal of Chemistry* 2016; **9**, S1155-S1162.

[21] L Nimah, SR Juliastuti and M Mahfud. Microwave-assisted synthesis, characterization, and performance assessment of lemongrass-derived activated carbon for removal of Fe and Mn from acid mine drainage. *Journal of Renewable Materials* 2025, **13(11)**, 2169-2190.

[22] G Wang, X Duan, D Wang, X Dong and X Zhang. Polyvinylidene fluoride effects on the electrocatalytic properties of air cathodes in microbial fuel cells. *Bioelectrochemistry* 2018; **120**, 138-144.

[23] CVVM Gopi, AE Reddy, JS Bak, IH Cho and HJ Kim. One-pot hydrothermal synthesis of tungsten diselenide/reduced graphene oxide composite as advanced electrode materials for supercapacitors. *Materials Letters* 2018; **223**, 57-60.

[24] LG Schultz. *Quantitative interpretation of mineralogical composition from X-ray and chemical data for the pierre shale*. United States Government Printing Office, Washington DC, 1964, p. C1-C31.

[25] C Choi, SD Seo, BK Kim and DW Kim. Enhanced lithium storage in hierarchically porous carbon derived from waste tea leaves. *Scientific Reports* 2016; **6(1)**, 39099.

[26] MAA Mariah, K Rovina, JM Vonnie and KH Erna. Characterization of activated carbon from waste tea (*Camellia sinensis*) using chemical activation for removal of methylene blue and cadmium ions. *South African Journal of Chemical Engineering* 2023; **44**, 113-122.

[27] RK Mishra, B Singh and B Acharya. A comprehensive review on activated carbon from pyrolysis of lignocellulosic biomass: An application for energy and the environment. *Carbon Resources Conversion* 2024; **7(4)**, 100228.

[28] AB Marahatta. XRD studies on metamorphic changes of the dissimilarly graphitized carbonaceous materials. *Asian Journal of Applied Chemistry Research* 2024; **15(4)**, 194-215.

[29] L Lestari, S Raharjo, IN Sudiana, LO Rusman and S Manikam. Production and characterization of microwave-activated palm kernel shell (*Elaeis Guineensis* Jacq.) activated charcoal. *Journal of World Science* 2024; **3(9)**, 1198-1207.

[30] E Taer, P Dewi, Sugianto, R Syech, R Taslim, Salomo, Y Susanti, A Purnama, Apriwandi, Agustino and RN Setiadi. The synthesis of carbon electrode supercapacitor from durian shell based on variations in the activation time. *AIP Conference Proceedings* 2018; **1927(1)**, 030026.

[31] A Vakili, AA Zinatizadeh, Z Rahimi, S Zinadini, P Mohammadi, S Azizi, A Karami and M Abdulgader. The impact of activation temperature and time on the characteristics and performance of agricultural waste-based activated carbons for

removing dye and residual COD from wastewater. *Journal of Cleaner Production* 2023; **382**, 134899.

[32] L Wu, D Xue, R Wen, X Jiang, L Jiao and H Chen. *Production of activated carbon from tea*. *In*: HS Min, HS Kusuma and YC Sharma (Eds.). Recent advances in activated carbon: synthesis, properties and applications, CRC Press, London, 2024, p. 13-26.

[33] S Bhoyate, CK Ranaweera, C Zhang, T Morey, M Hyatt, PK Kahol, M Ghimire, SR Mishra and RK Gupta. Eco-friendly and high performance supercapacitors for elevated temperature applications using recycled tea leaves. *Global Challenges* 2017; **1(8)**, 1700063.

[34] H Hasanah and H Aziz. Synthesis of activated carbon from waste tea by koh activation as high performance supercapacitors electrodes. *Journal of Chemical and Pharmaceutical Research* 2020; **12(6)**, 6-12.

[35] K Mensah-Darkwa, FO Agyemang, S Akromah, EK Arthur, F Abdallah and E Gikunoo. A comparative study on the performance of activated carbon electrodes and activated carbon/titanium dioxide nanotubes hybrid electrodes. *Scientific African* 2021; **12**, 00786.

[36] M Rosi, MNZ Fatmizal, DH Siburian, A Ismardi and NH Abdullah. Electrochemical properties of activated carbon electrodes for supercapacitor application: the effect of various electrolyte concentrations of Na2SO4. *Jurnal Ilmiah Pendidikan Fisika Al-Biruni* 2023; **12(2)**, 243-250.

[37] A Apriwandi, E Taer and R. Farma. Analysis of cyclic voltammetry dan galvanostatic charge discharge electrode supercapacitor based on activated carbon from Kepok Banana Leaf (Musa balbisiana). *Journal of Aceh Physics Society* 2021; **10(4)**, 94-101.

[38] Y Zhang, X Li, Z Li and F Yang. Evaluation of electrochemical performance of supercapacitors from equivalent circuits through cyclic voltammetry and galvanostatic charge/discharge. *Journal of Energy Storage* 2024; **86(A)**, 111122.

[39] M Mehmandoust, G Li and N Erk. Biomass-derived carbon materials as an emerging platform for advanced electrochemical sensors: recent advances and future perspectives. *Industrial & Engineering Chemistry Research* 2022; **62(11)**, 4628-4635.

[40] KKR Reddygunta, R Beresford, L Šiller, L Berlouis and A Ivaturi. Activated carbon utilization from corn derivatives for High-energy-density flexible supercapacitors. *Energy and Fuels* 2023; **37(23)**, 19248-19265.